THE JOURNAL OF BIOLOGICAL CHEMISTRY
Vol. 273, No. 33, Issue of August 14, pp. 21054–21060, 1998

Printed in U.S.A.

Novel Localization of a Na^+/H^+ Exchanger in a Late Endosomal Compartment of Yeast

IMPLICATIONS FOR VACUOLE BIOGENESIS*

(Received for publication, April 30, 1998)

Richard Nass and Rajini Rao‡

From the Department of Physiology, The Johns Hopkins University School of Medicine, Baltimore, Maryland 21205

Na^+/H^+ exchangers catalyze the electrically silent countertransport of Na^+ and H^+, controlling the transmembrane movement of salt, water, and acid-base equivalents, and are therefore critical for Na^+ tolerance, cell volume control, and pH regulation. In contrast to numerous well studied plasma membrane isoforms (*NHE1–4*), much less is known about intracellular Na^+/H^+ exchangers, and thus far no vertebrate isoform has been shown to have an exclusively endosomal distribution. In this context, we show that the yeast NHE homologue, Nhx1 (Nass, R., Cunningham, K. W., and Rao, R. (1997) *J. Biol. Chem.* 272, 26145–26152), localizes uniquely to prevacuolar compartments, equivalent to late endosomes of animal cells. In living yeast, we show that these compartments closely abut the vacuolar membrane in a striking bipolar distribution, suggesting that vacuole biogenesis occurs at distinct sites. Nhx1 is the founding member of a newly emergent cluster of exchanger homologues, from yeasts, worms, and humans that may share a common intracellular localization. By compartmentalizing Na^+, intracellular exchangers play an important role in halotolerance; furthermore, we hypothesize that salt and water movement into vesicles may regulate vesicle volume and pH and thus contribute to vacuole biogenesis.

Na^+/H^+ exchangers of eukaryotic cells comprise a family of membrane proteins catalyzing the electroneutral countertransport of Na^+ and H^+ (1–3). At the plasma membrane of animal cells, the prevailing Na^+ gradient generated by the Na^+/K^+-ATPase is used to drive H^+ equivalents from the cell. As such, these exchangers are involved in the regulation of intracellular pH, cell volume control, and transcellular Na^+ movements in epithelial tissue. These functions are closely related to physiological and pathophysiological cellular events, including fertilization, cell cycle control, differentiation, essential hypertension, gastric and kidney disease, and epilepsies. Na^+/H^+ exchange activity has been detected in virtually every cell type that has been examined, and at least six distinct NHE isoforms have been identified thus far. Molecular cloning of the first Na^+/H^+ exchanger (4) led to a predicted membrane topology based on the hydropathy profile of the amino acid sequence: there are 12 membrane-spanning segments comprising a discrete N-terminal structural domain of approximately 500 residues, followed by a long cytoplasmic C-terminal tail of approximately 300 residues. This predicted structural subdivision mimics a partition of function: analysis of deletion mutants has shown that the membrane-embedded domain retains the ability to insert into the plasma membrane, is transport-competent, and is sensitive to inhibition by amiloride and its derivatives (5). However, it is the C-terminal domain that carries multiple protein kinase consensus sites, binds calmodulin, and mediates the response to a multitude of regulatory signals involved in control of cell proliferation, volume, and osmolarity changes.

All Na^+/H^+ exchangers that have been characterized at a molecular level thus far localize predominantly, if not exclusively, to the plasma membrane. Nevertheless, there has been biochemical documentation of Na^+/H^+ exchange activity in endosomal preparations from kidney, liver, zymogen granules of pancreatic acinar cells, and chromaffin granules of adrenal glands (6–11). In each case, the exchange activity was reported to coexist with a distinct subset (~20%) of vesicles containing the vacuolar H^+-ATPase and to exhibit kinetic similarity with the plasma membrane exchangers with respect to reversibility, simple hyperbolic response to Na^+, and allosteric activation by H^+. However, amiloride did not inhibit the endocytic exchange activity, Li^+ was a poor substrate but a good inhibitor of Na^+/H^+ exchange, and the K_m for Na^+ was somewhat lower than that seen for plasma membrane isoforms (4.7–10 mM *versus* 15–18 mM), suggesting that the endocytic exchanger is a distinct molecular isoform.

In earlier work, we have shown that the *NHX1* gene of *Saccharomyces cerevisiae* mediates sequestration of Na^+ within an intracellular compartment, suggestive of a novel intracellular localization (12). Here, we provide direct evidence that Nhx1 localizes exclusively to a unique late endosomal compartment, thus providing a starting point to explore the molecular, cellular, and physiological functioning of a completely novel member of this family of transporters. We have also observed the emergence of new exchanger homologues in other organisms, as a result of systematic sequencing efforts worldwide, that share greater homology with yeast Nhx1 than to the plasma membrane isoforms. We suggest that the sequence similarites among these newly discovered isoforms is indicative of a common intracellular, possibly endosomal localization.

EXPERIMENTAL PROCEDURES

Yeast Strains and Recombinant DNA Techniques—Strains K601 (wild type) and R100 (Δ*nhx1*) used in this study are isogenic to W303 and have been described (12). A 4.5-kilobase pair (kbp)[1] *Sal*I insert containing the intact *NHX1* gene was recovered from cosmid C9410

* This work was supported by a grant from the National Institutes of Health and an American Cancer Society Junior Faculty Award (to R. R.). The costs of publication of this article were defrayed in part by the payment of page charges. This article must therefore be hereby marked "*advertisement*" in accordance with 18 U.S.C. Section 1734 solely to indicate this fact.

‡ To whom correspondence should be addressed: Dept. of Physiology, The Johns Hopkins University School of Medicine, 725 N. Wolfe St., Baltimore MD 21205. Tel.: 410-955-4732; Fax: 410-955-0461; E-mail: rajini_rao@qmail.bs.jhu.edu.

[1] The abbreviations used are: kbp, kilobase pair; PCR, polymerase chain reaction; HA, hemagglutinin; GFP, green fluorescent protein; PVC, prevacuolar compartment.

(American Type Culture Collection), and a 3-kbp *Sal*I to *Spe*I fragment from the 5′ portion of the gene was cloned into pRS425 (13), now called pRin72. The C terminus of Nhx1 was tagged with a triple hemagglutinin (HA) epitope using two polymerase chain reaction (PCR) products as primers for a third PCR. The following primers were used to amplify a 0.8-kbp product from cosmid C9410 that extended from +1.1 kbp downstream from the initiating ATG to the end of the *NHX1* open reading frame, with the removal of the termination codon, and addition of a *Not*I site and a short sequence homologous to the 5′ end of the HA epitope: 5′-CTGAAGTAGAACTAGTCTATAAGCCAC-3′ (sense) and 5′-AACATCGTATGGGTAAAAGATGCGGCCGCCGTGGTTTTGGGAAG-AGAAATCTGCAGG-3′ (antisense). The second PCR created a 1-kbp product beginning with a short sequence homologous to the 3′ end of the HA epitope, followed by the termination codon TAG, and extending through 1 kbp of 3′ noncoding sequence of the *NHX1* gene to a new *Sac*I site at the 3′ end. The following primers were used in conjunction with C9410 as template: 5′-GACGTTCCAGATTACGCTGCTGAGTGCTAG-CCGCGGGTAGACTTTAAAGTGTATGGTTTCC-3′ (sense) and 5′-GG-CACGAGCTCGTCTTCATCCATGACGGAAG-3′ (antisense). The final PCR reaction used the PCR products, above, as primers with the plasmid pSM491 (gift of Susan Michaelis, Johns Hopkins University) containing the triple HA epitope as the template. The resulting 1.9-kbp product was digested with *Spe*I and *Sac*I and cloned into pRin72 to give the full-length Nhx1::HA with the 1.9-kbp upstream sequence from the initiating codon ATG and the 1-kbp downstream sequence from the termination codon (pRin73). The Nhx1::GFP construct was created by digesting pEGFP-N3 (CLONTECH) with *Bam*HI and *Not*I to release the 0.7-kilobase GFP and ligating to the same sites in pRin72. To complete the *NHX1* open reading frame, a 1.3-kbp *Bam*HI fragment from pRin73 was inserted in the correct orientation into this plasmid, creating the full-length fusion.

Biochemical Methods—Assays of protein, α-mannosidase activity, Kex2 activity, and azide-sensitive ATPase activity have been described in earlier publications (14, 15) and in references therein. Differential centrifugation of yeast lysates and nonequilibrium fractionation of yeast lysates by sucrose gradient centrifugation was performed as described (14, 16). SDS-polyacrylamide gel electrophoresis and Western blotting were performed as described previously (14). Antibodies were used as follows: mouse anti-HA antibody, 12CA5 (Boehringer Mannheim) at 1:5000, mouse anti-Vph1, monoclonal antibody 10D7-A7-B2 (Molecular Probes) at 1:5000, mouse anti-Dpm1, monoclonal antibody 5C5-A7 (Molecular Probes) at 1:2500, mouse anti-GFP (Molecular Probes) at 1:500, rabbit anti-Pma1 (gift of Carolyn Slayman, Yale University) at 1:1000, rabbit anti-Pep12 (gift of Robert Piper, University of Iowa) at 1:1250, rabbit anti-Kex2 (gift of Robert Fuller, University of Michigan),at 1:1000. Horseradish peroxidase-coupled goat anti-mouse (Boehringer Mannheim) and horseradish peroxidase-coupled donkey anti-rabbit (Amersham Pharmacia Biotech) were used at 1:1000.

Confocal Microscopy—Cells (0.7–1.2 A_{600} units/ml) were labeled with 53 μM FM 4-64 (*N*-(3-triethylammoniumpropyl)-4-(6-(4-diethylamino)-phenyl)-hexatrienzyl)pyridinium dibromide), 13 nM $DiOC_6$ (3,3′-dihexyloxacarbocyanine iodide), and 40 nM MitoTracker Red CMXRos (all from Molecular Probes) using a variable labeling period (10–60 min) followed by chase in fresh medium (30–60 min). Confocal microscopy was performed by the Noran Oz Confocal Microscope System; single label controls for each fluorophore were captured under identical double label conditions to eliminate any fluorescence bleed-through.

RESULTS

Epitope-tagged and Plasmid-encoded Nhx1 Is Fully Functional and Induced by NaCl—Targeted disruption of the *S. cerevisiae NHX1* (YDR456w) gene leads to loss of sodium tolerance in acidic (Fig. 1*a*) but not neutral or alkaline medium (12), consistent with the expected properties of a H^+ driven Na^+ transporter. The *NHX1* gene was recovered from a 40-kilobase pair genomic insert in cosmid C9410 (see "Experimental Procedures"), and the open reading frame was tagged at the C terminus with either a triple HA epitope or the GFP. Expression of the tagged constructs was directed from the endogenous *NHX1* promoter in a Δ*nhx1* strain of yeast. Both tagged constructs appeared to be fully functional, effectively complementing the Na^+-sensitive phenotype of the Δ*nhx1* mutant in the single copy (*CEN*) as well as multicopy (2μ) plasmid versions (Fig. 1*a*). Like other members of the NHE family, yeast Nhx1 is predicted to be an integral membrane protein, with an N-terminal domain of 12 transmembrane helices, followed by a C-terminal cytoplasmic tail (12). Differential centrifugation of yeast lysates results in a substantial enrichment of Nhx1::HA (molecular mass, 73.5 kDa) in low speed membrane pellets (Fig. 1*b*); in the absence of further fractionation, the Nhx1 polypeptide characteristically migrates as multiple bands on SDS gels, indicative of post-translational modifications such as phosphorylation or glycosylation. Further evidence of the involvement of Nhx1 in halotolerance comes from salt induction of expression (Fig. 1*b*).

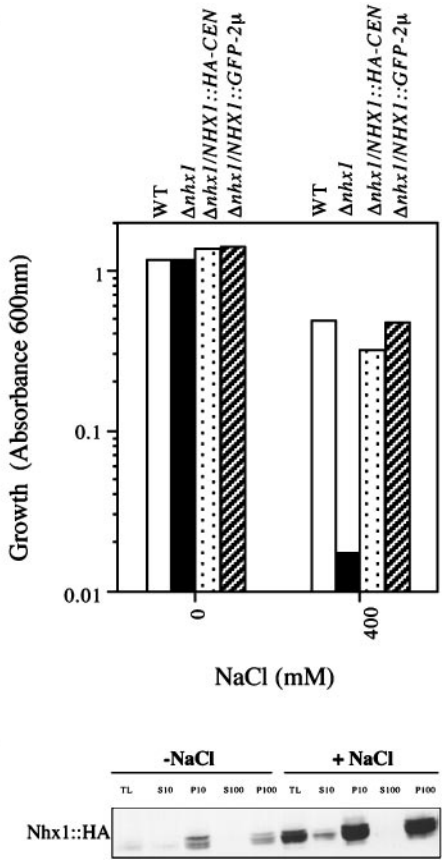

FIG. 1. **Epitope-tagged Nhx1 confers sodium tolerance and is induced by NaCl.** *a*, wild type (*WT*) or Δ*nhx1* strains of yeast carrying the plasmids as shown were grown to saturation at 30 °C in the absence or presence of 400 mM NaCl in APG medium, pH 4.0, as described previously (12). *b*, Δ*nhx1* cells expressing HA-tagged Nhx1 from its endogenous promoter in a 2μ plasmid (see "Experimental Procedures") were cultured in the absence or presence of NaCl (300 mM). Clarified lysates (*TL*) were divided into two aliquots and centrifuged at either 10,000 × *g* or 100,000 × *g*. Equal protein (90 μg) from pellet (*P*) or supernatant (*S*) fractions were subjected to SDS-polyacrylamide gel electrophoresis and Western blotting with anti-HA antibody. Note the increase in expression level in medium containing NaCl.

Colocalization of HA-tagged Nhx1 with Vacuolar and Prevacuolar Markers in Subcellular Fractions—Our measurements of steady state intracellular ^{22}Na levels indicated that enhanced sequestration of Na^+ via Nhx1 correlated with salt-tolerant growth (12). By analogy with observations of vacuolar compartmentation of salt in halotolerant plants (17, 18), we hypothesized that Na^+ transport by Nhx1 was likely to be coupled to the vacuolar H^+ pump in an acidic compartment. Here, we show that HA-tagged Nhx1 cofractionates with markers for the vacuole, prevacuolar compartment, and the late Golgi compartment on sucrose density gradients (Fig. 2*a*), whereas it clearly fractionated away from markers representing the endoplasmic reticulum, plasma membrane, and mitochondria, pointing to a hitherto novel cellular loca-

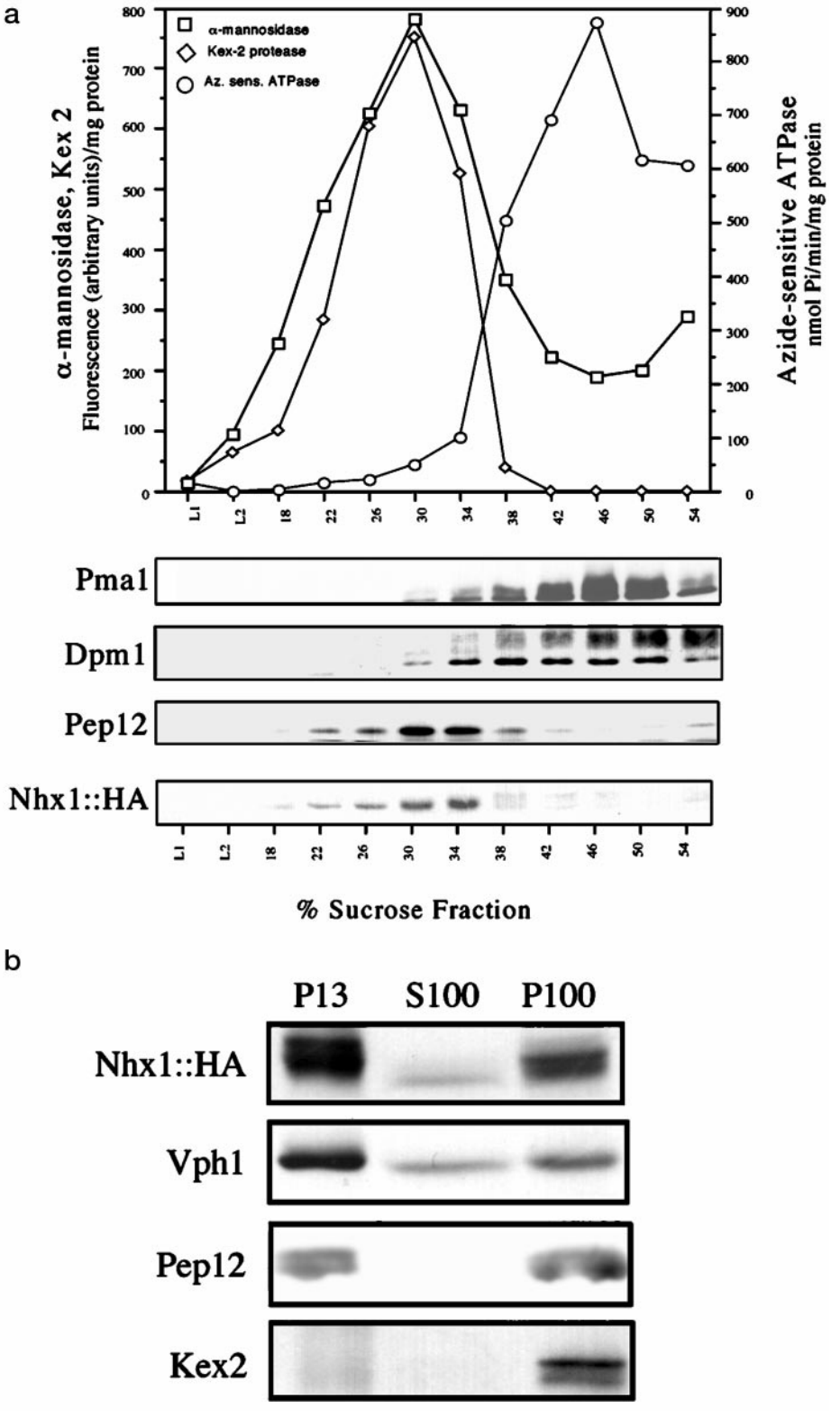

FIG. 2. **Subcellular fractionation of HA-tagged Nhx1.** *a*, Δ*nhx1* cells expressing HA-tagged Nhx1 (2μ) were grown in APG medium, converted to spheroplasts, lysed, and fractionated on a 10-step sucrose gradient (18–54% w/w), as described (14, 15). Fractions were assayed for enzymatic activity of markers of the vacuole (α-mannosidase), late Golgi (Kex2), and mitochondria (azide-sensitive F_1-ATPase). Western blots show the distribution of markers for the plasma membrane (*Pma1*, 20 μg/lane), endoplasmic reticulum (*Dpm1*, 20 μg/lane), prevacuolar compartment (*Pep12*, 20 μg/lane), and Nhx1::HA (90 μg/lane). *b*, yeast lysates from cells described in *a* were sequentially fractionated at 13,000 × *g* and 100,000 × *g* as described (16). Pellet fractions (*P*) were brought to the same volume as the supernatant (*S*), and equal volumes (0.03 ml) were subjected to gel electrophoresis and Western blotting as in *a*. Vph1 is a subunit of the vacuolar H^+-ATPase. Note that the distribution of Nhx1 is similar to that of Vph1 and Pep12 but different from that of Kex2.

tion for a Na^+/H^+ exchanger. To distinguish between prevacuolar, vacuolar, and Golgi distributions, subcellular fractions from sequential centrifugation of yeast lysates were analyzed by gel electrophoresis (Fig. 2*b*). Fractionation of Nhx1 closely followed that of the vacuolar marker, Vph1 (a subunit of the vacuolar H^+-ATPase), and that of Pep12 (a prevacuolar syntaxin) but was clearly different from the late Golgi protease, Kex2.

Confocal Microscopy of GFP-tagged Nhx1 Shows Localization to Unique, Bipolar Perivacuolar Compartments—To further define the cellular location of this novel exchanger, we used laser scanning confocal microscopy to examine the distribution of GFP-tagged Nhx1 in conjunction with the vacuolar stain FM 4-64 in exponentially growing, unfixed cells (Fig. 3). Fluorescence from Nhx1::GFP appears as 1–2 intensely fluorescent spots per cell, immediately abutting the vacuolar membrane, usually with a striking bipolar distribution. The number and size of the spots typically increase in salt-containing me-

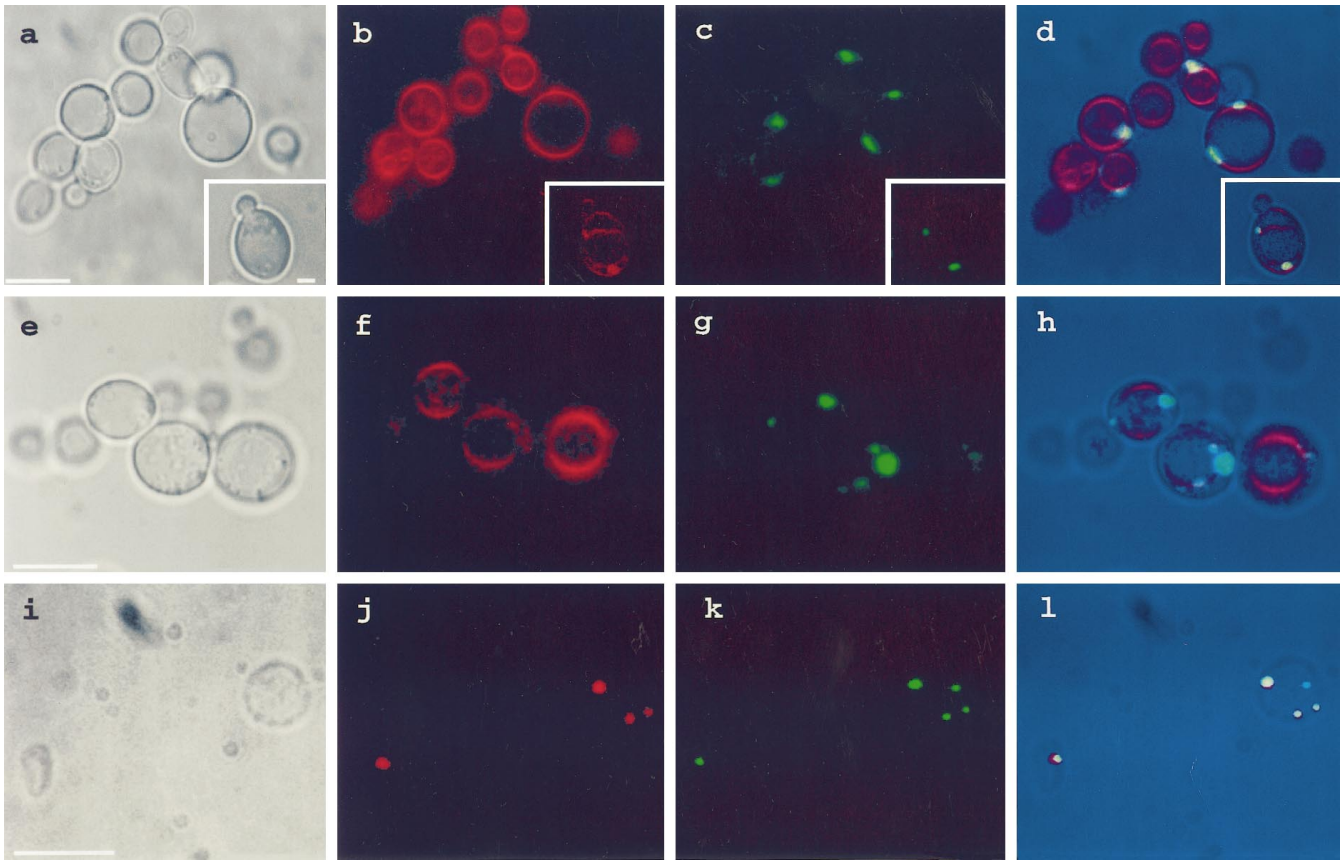

FIG. 3. **Confocal microscopy of GFP-tagged Nhx1.** Confocal images of exponentially growing, unfixed cells of Δ*nhx1* carrying the Nhx1::GFP (2μ) construct (see "Experimental Procedures") in the absence (*a–d*) or presence (*e–h*) of 300 mM NaCl. Contrast images of living yeast cells are shown in *panels a* and *e*. Vacuoles are stained *red* with FM 4-64 (*panels b* and *f*). Nhx1::GFP fluorescence appears as one or two intense *green* spots per cell (*panels c* and *g*) that always are directly abutting the vacuolar membrane, often bipolar in orientation relative to the vacuole (*inset*, *panel c*). The three images are overlaid in *panels d* and *h*. In fixed and permeabilized cells (*I–l*), indirect immunofluorescence from antibodies against Pep12 (*panel j*, *red*), a resident of the prevacuolar compartment, colocalize with Nhx1::GFP fluorescence (*panel k*, *green*), as seen in the overlay (*panel l*). *Bar*, 10 μm; *inset bar*, 2 μm.

dia, consistent with the observed induction of Nhx1 expression levels. The distinct perivacuolar location of the signal is highly reminiscent of the prevacuolar compartment (19, 20), at which the biosynthetic, autophagic, and endosomal pathways converge for sorting of cargo before final delivery to the vacuole. Indeed, we show that the syntaxin Pep12, which defines the identity of the prevacuolar compartment (21), colocalizes with Nhx1::GFP in fixed and permeabilized cells. Importantly, we were able to show by Western blotting using anti-GFP antibodies that the distribution of Nhx1::GFP was identical to that of Nhx1::HA on sucrose density gradients (data not shown). Together with the functionality of the tagged constructs (Fig. 1*a*) and the modest levels of expression achieved from the endogenous *NHX1* promoter, the observations argue against a potential mislocalization because of the large GFP tag.

The frequent distribution of Nhx1::GFP to opposing ends or poles of the vacuole is particularly intriguing and was clearly observed in three-dimensional reconstructions of the vacuole from sequential confocal planes (not shown). Such a bipolar pattern recalls the similar "patched" distribution of vacuolar assembly proteins, Vam3 and Vam6, on the vacuolar membranes (34, 35) and suggests that fusion of vacuolar precursors occurs at discrete sites. We note that this orientation is apparently lost upon fixation of cells.

Nhx1 Does Not Colocalize with Mitochondrial Markers—The inner membrane of mitochondria in mammals has been shown to possess two distinct forms of cation/H^+ exchange activity: one selective for Na^+ and the other transporting all alkali cations (22, 23). Functional studies in isolated yeast mitochondria indicate an absence of selective Na^+/H^+ exchange, although a nonselective (K^+/H^+) antiporter was found (24). A very recent report (25) raised the possibility that Nhx1 localizes to mitochondria based on an overlap of signals from the DNA-binding dye 4′,6′-diaminidino-2-phenylindole dihydrochloride and Nhx1::GFP expressed at high levels from the exogenous *MET25* promoter. Evidence was also presented for low levels (1 nmol/min/mg) of Na^+/H^+ exchange activity in three of five crude mitochondrial preparations, although contamination by other membranes was not assessed. Here we show that fluorescence from Nhx1::GFP is distinct from that of two well characterized mitochondrial dyes, $DiOC_6$ and MitoTracker Red CMXRos (Fig. 4). Mitochondria appear as typically elongated snake-like forms that have no particular orientation relative to the vacuole; in contrast, Nhx1::GFP flurorescence occurs as 1–2 spots/cell that are always observed to directly abut the vacuolar membrane. Taken together with the results from subcellular fractionation (Fig. 2*a*), we conclusively rule out a mitochondrial localization for this exchanger.

DISCUSSION

Nhx1 Defines a Novel Cluster of Na^+/H^+ Exchanger Isoforms—With the ongoing success of systematic genome sequencing, genes encoding putative Na^+/H^+ exchangers have recently been identified in yeasts, worms, bacteria, and humans. They provide a unique opportunity to trace the phylogenetic ancestry and evolution of exchanger isoforms as well as

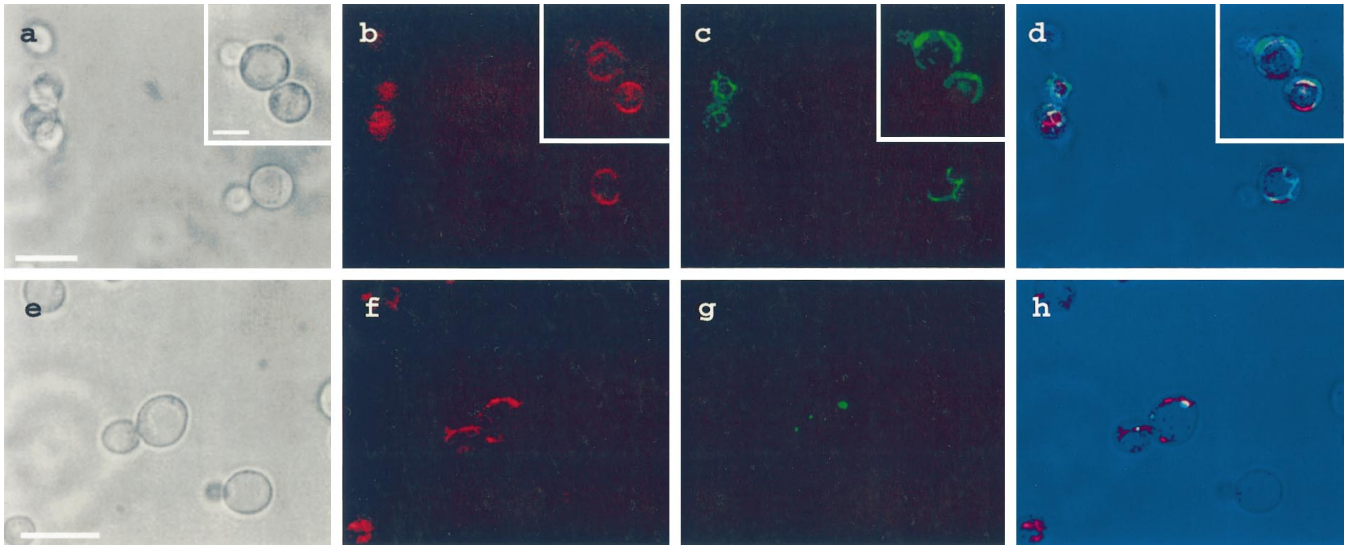

FIG. 4. **Nhx1 does not colocalize with mitochondrial markers.** Confocal microscopy of exponentially growing wild type (*panels a–d*) or Δ*nhx1*/Nhx1::GFP-2μ (*panels e–h*) cells in the absence of fixation. In *panels a–d*, mitochondria stained with $DiOC_6$ (*green*, *panel c*) are seen in relation to the vacuole (FM 4-64; *red*, *panel b*) in the overlay (*panel d*). Nhx1::GFP fluorescence (*panel g*) is distinct from that of mitochondria (MitoTracker Red CMXRos; *red*, *panel f*) as seen in the overlay (*panel h*). Note that mitochondria lack the distinct perivacuolar, bipolar distribution seen in the structures containing Nhx1::GFP. *Bar*, 10 μm; *inset bar*, 5 μm.

provide clues to the function of newly identified homologues. In our survey of all NHE-like sequences residing in data bases, we were able to identify previously known clusters of sequences corresponding to the plasma membrane isoforms of Na^+/H^+ exchangers (NHE1–4), as well as a previously unreported cluster of more distantly related prokaryotic sequences. We show here that Nhx1 defines a completely novel cluster of exchanger sequences derived from such evolutionary divergent organisms as yeast, nematodes, and humans (Fig. 5*a*). In addition, pairwise comparisons between NHE polypeptides using global alignment methods (26) reveal significantly higher scores for members within this newly identified cluster: average identity, 34%; global score, 1000 (*Box I*, Fig. 5*b*). Comparable scores were observed among members outside this cluster: average identity, 36%; global score, 1722 (*Box II*, Fig. 5*b*). In contrast, scores for sequence pairs *between* the two groups were uniformly low: average identity, 23%; global score, 373 (*Box III*, Fig. 5*b*). It should be noted that to avoid bias, we chose representative sequences from widely divergent phyla in both groups and that the overall length of the polypeptides varied in both groups: 540–666 (*Box I*) and 660–820 (*Box II*).

All Na^+/H^+ exchanger sequences share the highest homology within predicted transmembrane segments of the N-terminal transporter domain. The conserved regions are presumably important for common transport functions, whereas the C-terminal domains are largely divergent, reflecting a diversity in modes of regulation of different isoforms. In Fig. 5*c*, we show that there are consistent differences between members of the different clusters in sequence homology patterns within transmembrane segments known to be important for amiloride binding and ion transport. On the basis of these differences we suggest that members of the Nhx1-like cluster diverged early from plasma membrane isoforms. Finally, the length of the C-terminal hydrophilic domain is significantly shorter in members of the Nhx1-like cluster relative to the plasma membrane isoforms, resulting in shorter polypeptide lengths overall: 541–666 residues *versus* 717–832 residues. Thus, although separated from one another by a billion years or so of evolution, members of the newly identified Nhx1-like cluster are all recognizably related to each other. Taken together, these observations suggest a common intracellular, possibly endosomal location for these novel homologues.

Functional Implications of the Prevacuolar/Endosomal Localization of Nhx1—There is emerging evidence that plasma membrane-derived endosomes and Golgi-derived transport vesicles converge at a prevacuolar compartment (PVC) equivalent to late endosomes, where cargo is sorted prior to final delivery to the vacuole/lysosome. Proteins *en route* to the vacuole may be visualized in the PVC transiently, as was observed for the α-factor receptor, Ste3, upon coordinated internalization from the plasma membrane (27), or by perturbation of vesicle traffic into or out of this compartment, as in the "Class E" family of vacuolar trafficking mutants (28). The PVC itself is a discrete, rather than transient, structure that can be isolated on density gradients from normal yeast (29) and can be shown to have a perivacuolar distribution by immunofluorescence and electron microscopy (20, 27). However, the only resident protein of the PVC described in the literature is the syntaxin homologue, Pep12, which mediates docking of this compartment with the vacuole (21). In this context, the selective localization of Nhx1 to the prevacuolar compartment has considerable functional significance. An intriguing possibility is that regulation of vesicle volume and pH by endosomal Na^+/H^+ exchange may be important for vacuole biogenesis. Thus, the H^+ gradient established by the vacuolar H^+-ATPase would drive Na^+ accumulation via Na^+/H^+ exchange, and Cl^- influx via chloride channels (Fig. 5*d*). As osmotically obliged water is dragged in, the vesicle swells and the hydrostatic pressure generated provides the energy for membrane destabilization and fusion. There is evidence that osmotic swelling precedes exocytosis and that, conversely, water loss from vesicles accompanies vesicle maturation and remodeling (30–32, 39). We suggest that the yeast chloride channel ScCLC/GEF1 also has a prevacuolar localization based on the appearance of GFP-tagged ScCLC as 1–3 perivacuolar dots/cell (33). Thus, colocalization of the Na^+/H^+ exchanger, Cl^- channel, and H^+ pump, together with specialized coat proteins, syntaxins, and other docking factors may be involved in the assembly of the vacuole/lysosome from the prevacuolar compartment/endosomes.

Our data do not exclude the possibility that Nhx1 also localizes to discrete patches on the vacuolar membrane. Recently, two components of a protein complex required for vacuole biogenesis, Vam3 (34) and Vam6 (35), were shown to have an unusual bipolar patched location on the vacuole, suggesting

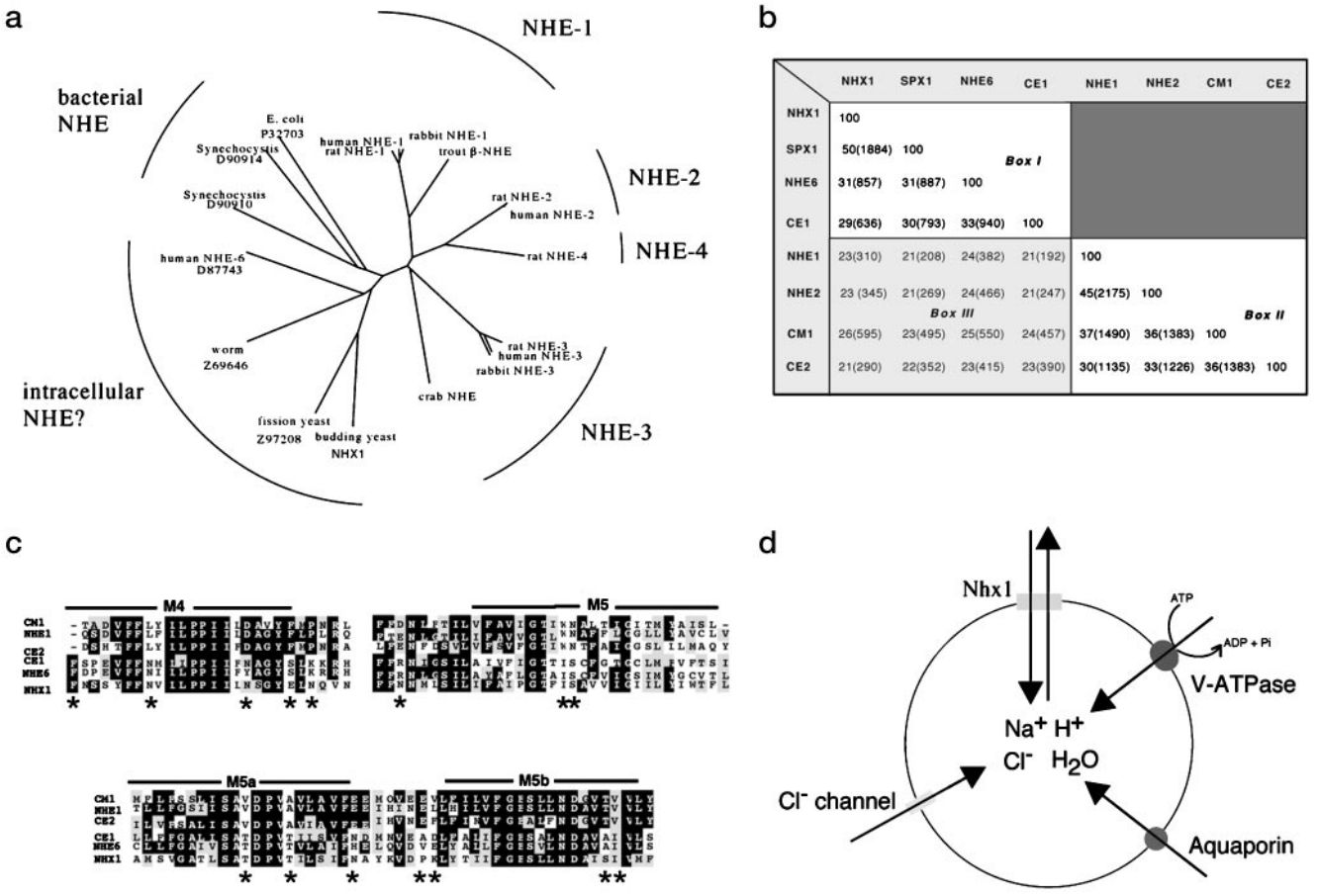

FIG. 5. **Sequence relations and proposed function of Nhx1-like homologues.** *a*, phylogenetic clusters of NHE sequences were defined using Clustalw 1.5 and PHYLIP 3.5c. Representative examples are shown for each cluster, and accession numbers are included for unnamed isoforms. *b*, pairwise alignments between NHE sequences showing the percentage of identity computed for each pair. In *parentheses* are the global alignment scores, which reflect penalties for gaps. *Box I* contains the putative intracellular cluster, and *Box II* contains representative examples from the other clusters. *NHX1*, *S. cerevisiae*; *SPX1*, *S. pombe* Z97208; *NHE6*, human D87743; *CE1* and *CE2*, *C. elegans* Z69646 and Z73898); *NHE1*, rat; *NHE2*, human; *CM1*, *C. maenas*. *c*, patterns of amino acid homology provide the basis for the definition of unique clusters of NHE sequences. Selected transmembrane segments are shown, numbered according to Ref. 1. *Asterisks* highlight the differences between putative intracellular isoforms and other NHE sequences. *d*, model for salt and water accumulation in vesicles. A specific colocalization of the transporters depicted has not yet been shown but is likely. Swelling of the vesicles is proposed to precede fusion of the prevacuolar compartment with the vacuole.

that specialized domains of the vacuole may be involved in vesicle fusion. By analogy, it is known that Golgi-derived secretory vesicles fuse at specialized regions of the plasma membrane, resulting in oriented bud growth (36). We note the enrichment of mammalian *Nhe*I at the leading edge and ruffles in fibroblast cells (37), and of the unrelated Na^+/H^+ exchanger sod2 of *Schizosaccharomyces pombe* to the polarized cell tips (38), consistent with a role for Na^+/H^+ exchange at these specialized sites. Our data imply that regulation of vesicle pH and volume by endosomal Na^+/H^+ exchange may be important for vesicle maturation and fusion.

Given the multifunctionality of Na^+/H^+ exchangers, a variety of other cellular roles for endosomal exchangers may be envisaged: regulation of endosomal pH via Na^+/H^+ exchange can provide a functional link between the operational diversity among endocytic compartments and the known variability in their internal pH, intralumenal sequestration of Na^+ may serve to detoxify the cytoplasm or to drive Ca^{2+} accumulation via Na^+/Ca^{2+} exchange, and in the case of the renal proximal tubule, exocytic insertion of endosomal Na^+/H^+ exchangers at the cell surface may effect rapid increases in H^+ secretory capacity. We have already demonstrated that in yeast, Nhx1 makes an important contribution to halotolerance (12). The molecular characterization and functional role of Nhx1-like homologues in other organisms remains to be determined.

Acknowledgments—We thank Robert Fuller, Robert Piper, and Carolyn Slayman for generous gifts of antibody and acknowledge the experimental contributions of Emily Corse and Patrick Leibovich. Michael Delannoy and Oliver Kerscher provided helpful advice for microscopy.

REFERENCES

1. Wakabayashi, S., Shigekawa, M., and Pouyssegur, J. (1997) *Physiol. Rev.* **77,** 51–74
2. Tse, C.-M., Levine, S. A., Brant, S. R., Nath, S., Pouyssegur, J., and Donowitz, M. (1994) *Cell. Physiol. Biochem.* **4,** 282–300
3. Orlowski, J., and Grinstein, S. (1997) *J. Biol. Chem.* **272,** 22373–22376
4. Sardet, C., Franchi, A., and Pouyssegur, J. (1989) *Cell* **56,** 271–280
5. Wakabayashi, S., Fafournoux, P., Sardet, C., and Pouyssegur, J. (1992) *Proc. Natl. Acad. Sci. U. S. A.* **89,** 2424–2428
6. Gurich, R. W., and Warnock, D. G. (1986) *Am. J. Physiol.* **251,** F702–F709
7. Hilden, S. A., Ghoshroy, K. B., and Madias, N. E. (1990) *Am. J. Physiol.* **258,** F1311–F1319
8. Hensley, C., Bradley, M., and Mircheff, A. K. (1990) *Kidney Int.* **37,** 707–716
9. Van Dyke, R. W. (1995) *Am. J. Physiol.* **269,** C943–C954
10. Thevenod, A. F. (1996) *J. Membr. Biol.* **152,** 195–205
11. Haigh, J. R., and Phillips, J. H. (1989) *Biochem. J.* **257,** 499–507
12. Nass, R., Cunningham, K. W., and Rao, R. (1997) *J. Biol. Chem.* **272,** 26145–26152
13. Christianson, T. W., Sikorski, R. S., Dante, M., Shero, J. H., and Hieter, P. (1992) *Gene* (*Amst.*) **110,** 119–122
14. Sorin, A. G., Rosas, G., and Rao, R. (1997) *J. Biol. Chem.* **272,** 9895–9901
15. Antebi, A., and Fink, G. R. (1992) *Mol. Biol. Cell* **3,** 633–654
16. Becherer, K. A., Rieder, S. E., Emr, S. D., and Jones, E. W. (1996) *Mol. Biol. Cell* **7,** 579–594
17. Serrano, R. (1996) *Int. Rev. Cytol.* **165,** 1–52
18. Barkla, B. J., Apse, M. P., Manolson, M. F., and Blumwald, E. (1994) *Symp. Soc. Exp. Biol.* **48,** 141–153
19. Raymond, C. K., Howald-Stevenson, I., Vater, C. A., and Stevens, T. H. (1992)

Mol. Biol. Cell **3,** 1389–1402
20. Rieder, S. E., Banta, L. M., Kohrer, K., McCaffery, J. M., and Emr. S. D. (1996) *Mol. Biol. Cell* **7,** 985–999
21. Becherer, K. A., Rieder, S. E., Emr, S. D., and Jones, E. W. (1996) *Mol. Biol. Cell* **7,** 579–594
22. Garlid, K. D., Shariat-Madar, Z., Nath, S., and Jezek, P. (1991) *J. Biol. Chem.* **266,** 6518–6523
23. Garlid, K. D. (1978) *Biochem. Biophys. Res. Commun.* **83,** 1450–1455
24. Welihinda, A. A., Trumbly, R. J., Garlid, K. D., and Beavis, A. D. (1993) *Biochim. Biophys. Acta* **1144,** 367–373
25. Numata, M., Petrecca, K., Lake N., and Orlowski, J. (1998) *J. Biol. Chem.* **273,** 6951–6959
26. Pearson, W. R. (1990) *Methods Enzymol.* **183,** 63–98
27. Hicke, L., Zanolari, B., Pypaert, M., Rohrer, J., and Riezman, H. (1997) *Mol. Biol. Cell* **8,** 13–31
28. Piper, R. C., Cooper, A. A., Yang, H., and Stevens, T. H. (1995)*J. Cell Biol.* **131,** 603–617
29. Darsow, T., Rieder, S. E., and Emr, S. D. (1997) *J. Cell Biol.* **138,** 517–529
30. Satir, B., Schooley, C., and Satir, P. (1973) *J. Cell Biol.* **56,** 153–176
31. Griffiths, G., Back, R., and Marsh, M. (1989) *J. Cell Biol.* **90,** 40–54
32. Scharschmidt, B. F., Lake, J. R., Renner, E. L., Licko, V., and Van Dyke, R. W. (1986) *Proc. Natl. Acad. Sci. U. S. A.* **83,** 9488–9494
33. Hechenberger, M., Schwappach, B., Fischer, W. N., Frommer, W. B., Jentsch, T. J., and Steinmeyer, K. (1996) *J. Biol. Chem.* **271,** 33632–33638
34. Wada, Y., Nakamura, N., Ohsumi, Y., and Hirata, A. (1997) *J. Cell Sci.* **110,** 1299–1306
35. Nakamura, N., Hirata, A., Ohsumi, Y., and Wada, Y. (1997) *J. Biol. Chem.* **272,** 11344–11349
36. TerBush, D. R., and Novick, P. (1995) *J. Cell Biol.* **130,** 299–312
37. Grinstein, S., Woodside, M., Waddell, T. K., Downey, G. P., Orlowski, J., Pouyssegur, J., Wong, D. C. P, and Foskett, J. K. (1993) *EMBO J.* **12,** 5209–5218
38. Dibrov., P., Smith, J. J., Young, P. G., and Fliegel, L. (1997) *FEBS Lett.* **405,** 119–124
39. Grinstein, S., Vander Meulen, J., and Furuya, W. (1982) *FEBS Lett.* **148,** 1–4